PROCEEDINGS OF SCIENCE

Near prospects for flavour physics

Andrey Golutvin*
Imperial College London, ITEP Moscow, CERN
E-mail: andrey.goloutvin@cern.ch

A selective summary of the the Beauty 2011 conference is presented with a particular emphasis given to the prospects to discover New Physics in heavy flavour experiments in the near future.

The 13th International Conference on B-physics at Hadron Machines - BEAUTY 2011,
April 4-8, 2011
Amsterdam, Netherlands

*Speaker.

PoS(BEAUTY 2011)021

The goal of this summary is to give a brief overview of the prospects in the near future (∼5 years for discovering New Physics (NP) in heavy flavour decays using indirect methods. For the next few years, at least, flavour physics will be dominated by the LHC. Already it is possible to give reliable predictions of the reach of the LHC flavour physics programme, thanks to the excellent start-up of the machine and the good performance demonstrated by the detectors [1, 2, 3, 4]. Large samples of high quality data are being accumulated at the LHC. These samples will substantially increase the sensitivity of indirect searches for NP in processes mediated by loop diagrams. Moreover, besides providing a further increase of accuracy in already well measured parameters, a new class of observables should soon become accessible. These observables will allow very stringent tests of the Standard Model (SM) to be performed separately in box diagrams and in penguin diagrams, involving quarks of all three generations. These tests require thorough exploration of both the beauty and the charm sector.

A search strategy is being developed on an illustrative set of "key measurements" sensitive to the phases and couplings of NP and even to their helicity structure. The main objectives addressed by flavour physics experiments include:

- A measurement of the B_s mixing phase, ϕ_s, in $B_s^0 \to J/\psi(\mu\mu)\phi(KK)$ decays;
- A measurement of the Unitarity Triangle (UT) angle γ in the processes mediated by tree diagrams using both time-integrated and time-dependent CP-violation measurements. These include studies of decays of the type $B^+ \to D^0 K^+$, $B_d^0 \to D^0 K^{*0}$, $B_d^0 \to D^{(*)}\pi$ and $B_s^0 \to D_s K$;
- A measurement of the UT angle γ in loop mediated processes. The $B_{d,s}^0 \to h^+h^-$ family of decays, where h stands for a pion or kaon, has decay rates with sizable contribution from penguin diagrams, making them sensitive to NP effects in penguin loops;
- A search for the super-rare $B_s^0 \to \mu^+\mu^-$ decay;
- A test of the $V-A$ helicity structure of the weak interaction in loop mediated $B_d^0 \to K^{*0}\mu^+\mu^-$ decays;
- A search for CP-violating asymmetries in charm decays.

1. Performance of the LHC detectors validated with data

The key features of detector performance relevant to heavy flavour physics are excellent vertex and impact parameter resolution, high track reconstruction and particle identification efficiency, superior mass resolution, proper time resolution and flavour tagging, and a flexible trigger which effectively selects particles produced in the decays of heavy flavours.

Vertexing and tracking

The large Impact Parameter (IP) of the track with respect to the interaction vertex is a distinctive feature to identify heavy flavour particle decays. Amongst the LHC detectors, the best IP resolution has been achieved by LHCb [4] as shown in Figure 1 (left). The resolution of 14 μm in the highest P_t bin agrees very well with the Monte Carlo expectation. Closely related to the IP

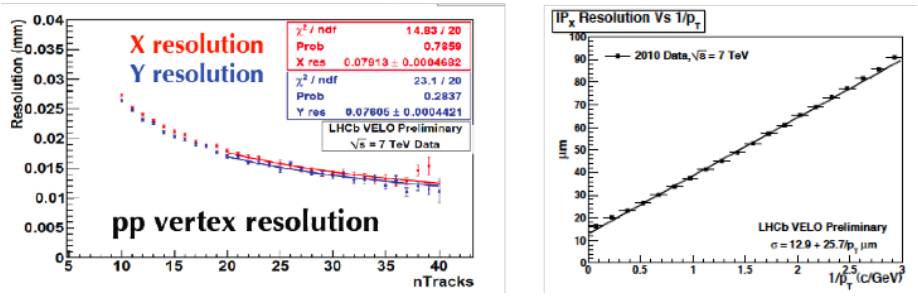

Figure 1: The left hand histogram shows the LHCb primary vertex resolution in the X- and Y projections versus the number of tracks originated from the vertex. The right hand histogram shows the LHCb IP_X resolution as a function of $1/P_t$.

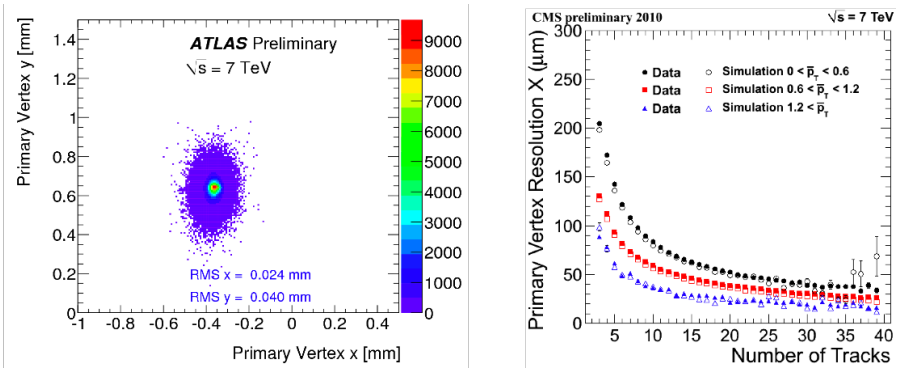

Figure 2: The left hand plot shows the two-dimensional distribution of the ATLAS primary vertex resolution in the X-Y transversal plane. The right hand histogram shows the CMS primary vertex resolution in the X projection versus the number of tracks originated from the vertex.

resolution is the vertex resolution which is a quantity crucial for the proper time reconstruction and for separating vertices from multiple interactions. Vertex resolutions have been measured by randomly splitting all reconstructed tracks into two subsets and by reconstructing vertices from each of the subsets. For a typical pp vertex producing 25 tracks the LHCb resolution has been found to be 15 μm in transverse plane, as shown in Figure 1 (right), and 75 μm along the beam line [4]. The primary vertex resolutions achieved by ATLAS [2] and CMS [3] are shown in Figure 2 (left) and (right) correspondingly. For primary vertices reconstructed from more than 10 tracks with average $P_t > 1.2$ GeV the resolution is close to 20μm in transverse plane as demonstrated by CMS.

Recent progress in the spectrometer alignment and calibration of the momentum resolution is reflected in the improved agreement between data and Monte Carlo for the invariant mass resolution measured for selected benchmark decays. Various B hadron species, as reconstructed by LHCb in $J/\psi X$ final states [5, 6] are shown in Figure 3. The signal-to-background ratio is comparable to similar signals seen at the B-factories in the e^+e^- environment. The invariant mass resolution for the golden $B_s \to J/\psi\phi$ decay is as good as 7 MeV/c^2. Somewhat worse invariant mass resolutions of 26 MeV/c^2 [7] and 16 MeV/c^2 [8] have been demonstrated by the ATLAS and CMS detectors respectively, as shown in Figure 4. As expected, in the relatively low momentum region of the J/ψ decay products in ATLAS and CMS compared to LHCb multiple scattering dominates the invariant

mass resolution leading to a modest degradation.

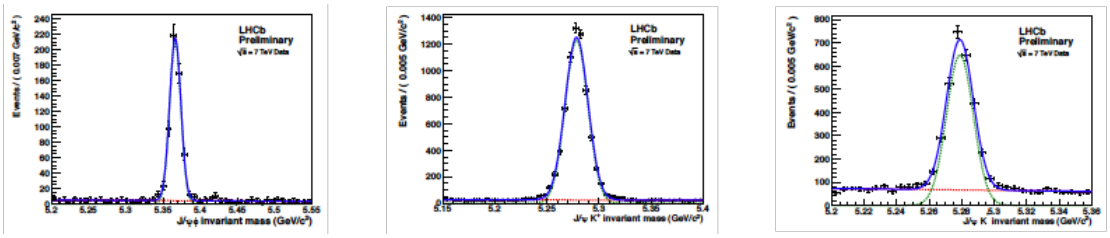

Figure 3: The LHCb $J/\psi X$ invariant mass distributions in the $B_{d,s}$ region for the $J/\psi\phi$, $J/\psi K^*$ and $J/\psi K^+$ final states.

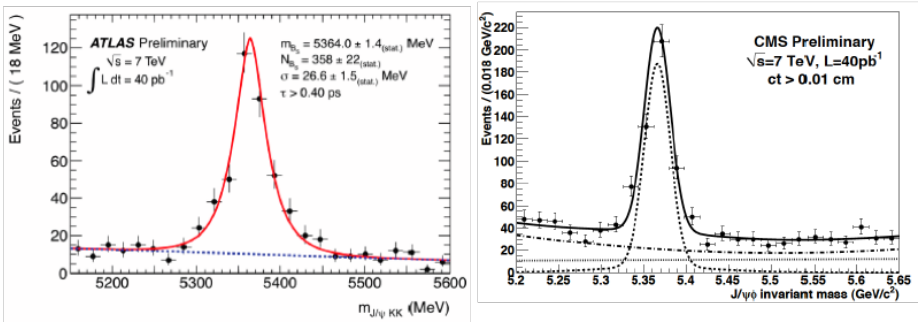

Figure 4: The $J/\psi\phi$ invariant mass distributions in the B_s region as achieved by ATLAS (left) and CMS (right).

Particle identification

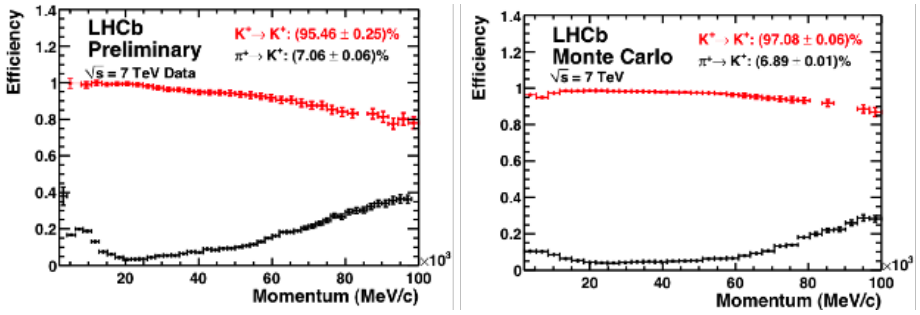

Figure 5: The histogram shows the LHCb RICH π/K separation performance as a function of the track momentum for data (left) and Monte Carlo (right).

Excellent identification of leptons and hadrons is fundamental for the reconstruction of heavy flavour decays. The LHCb RICH detectors provide unique capability to separate between protons, kaons and pions in the momentum range from 2 up to 100 GeV/c. The performance of pion and proton identification has been studied using the daughter particles of reconstructed K_S mesons and Λ baryons. For kaons, the reconstructed $\phi \to K^+K^-$ and $D^0 \to K\pi$ decays have been used.

In the former case, identifying only a single track using RICH information, and leaving the other unbiased, yields a sufficiently pure sample that can be used to measure the kaon identification

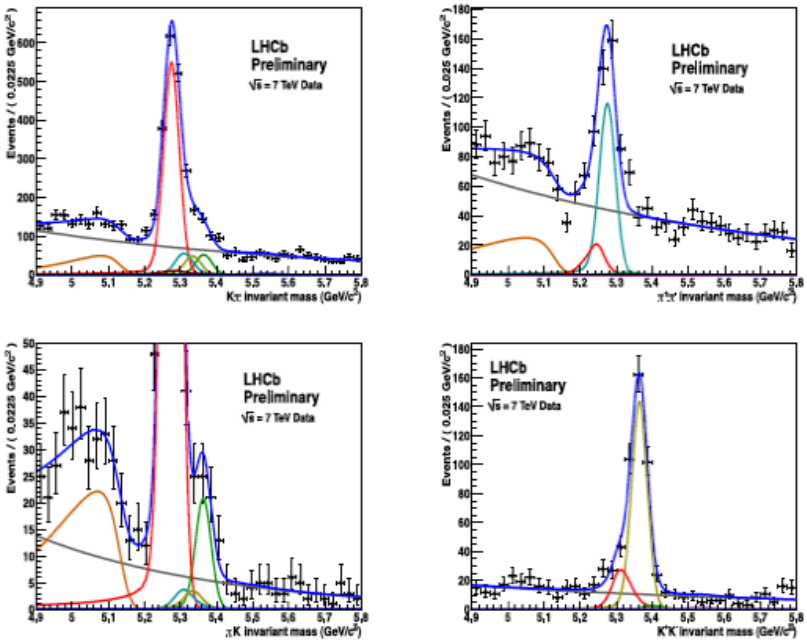

Figure 6: LHCb invariant mass spectra for $B^0 \to K^+\pi^-$ (top, left), $B^0 \to \pi^+\pi^-$ (top, right), $B_s \to \pi^+K^-$ (bottom, left, green line), and $B_s \to K^+K^-$ (bottom, right).

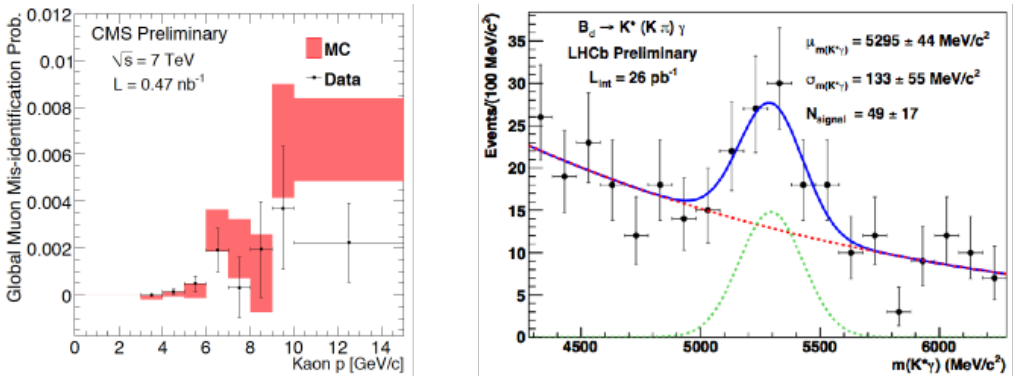

Figure 7: The left hand histogram shows the CMS $K-\mu$ misidentification probability as a function of the K momentum. The right hand histogram shows the LHCb $K^{*0}\gamma$ invariant mass distribution in the B_d mass region.

efficiency. In the latter, the kinematics of the $D^* \to D^0\pi$ decay allows pure samples to be isolated without recourse the PID information. The K/π separation performance currently achieved [4] (see Figure 5 (left)) is in good agreement with the Monte Carlo expectation shown in Figure 5 (right). The best performance is achieved in the momentum range from 5 to 70 GeV/c where most hadrons from b decays are produced. The LHCb RICH enables clean reconstruction of various hadronic $B_{(s)}$ and $D_{(s)}$ decays as illustrated in Figure 6 for the $B^0 \to K^+\pi^-$, $B^0 \to \pi^+\pi^-$, $B_s^0 \to \pi^+K^-$ and $B_s^0 \to K^+K^-$ final states [9].

All LHC detectors have demonstrated excellent muon, electron and photon identification capabilities. Muons are identified with close to 100% efficiency and with a misidentification rate below

the 1% level, saturated by the K decays in flight. CMS has excellent matching capability between the track segments measured by the tracking stations inside the solenoid and the muon chambers, which lie in the region of the return field. This feature allows the $K-\mu$ misidentification rate to be as low as $\sim$0.2% [3], as shown in Figure 7 (left).

Electron and photon identification is mainly based on the balance of the energy deposited in the calorimeter system and the track momentum, and the matching between the corrected barycenter position of the calorimeter cluster and the extrapolated track impact point. The electromagnetic calorimeters of the LHC detectors have been calibrated to $\sim$2% accuracy and enable an important extensions to the heavy flavour physics programme. As an example, Figure 7 (right) shows the signal for radiative $B \to K^*\gamma$ decays as reconstructed in LHCb, with the invariant mass resolution consistent with the Monte Carlo expectation [10].

Proper time resolution and flavour tagging

Excellent proper-time resolution is critical to the time-dependent measurements in the $B_s - \bar{B}_s$ meson system in order to be able to resolve its very fast oscillations. The proper decay time resolution leads to a dilution of the oscillation amplitude and consequently worsens the sensitivity. LHCb has measured its proper time resolution to be $\sim$50 fs [6] (see Figure 8 (left)) using a large data sample of the $J/\psi \to \mu^+\mu^-$ decays accumulated with the life time unbiased trigger. For comparison the CDF proper time resolution is a factor of 2 worse. Neither ATLAS nor CMS reported a measurement of the proper time resolution at this conference.

The flavour tagging performance of LHCb has been optimised using various flavour specific channels such as $B^0 \to D^{*+}\mu^-\nu$, $B^+ \to J/\psi K^+$ and $B^0 \to J/\psi K^{*0}$. The tagging power of the opposite side tagging was measured to be $2.2 \pm 0.5\%$ [5].

The tagging performance of LHCb has been validated by the world′s best measurement of the $B_s - \bar{B}_s$ oscillation frequency in the $B_s \to D_s\pi$ channel, $\Delta m_s = 17.63 \pm 0.11 \pm 0.04$ ps [5]. The mixing asymmetry for B_s signal candidates as a function of proper time modulo $2\pi/\Delta m_s$ is shown in Figure 8 (right).

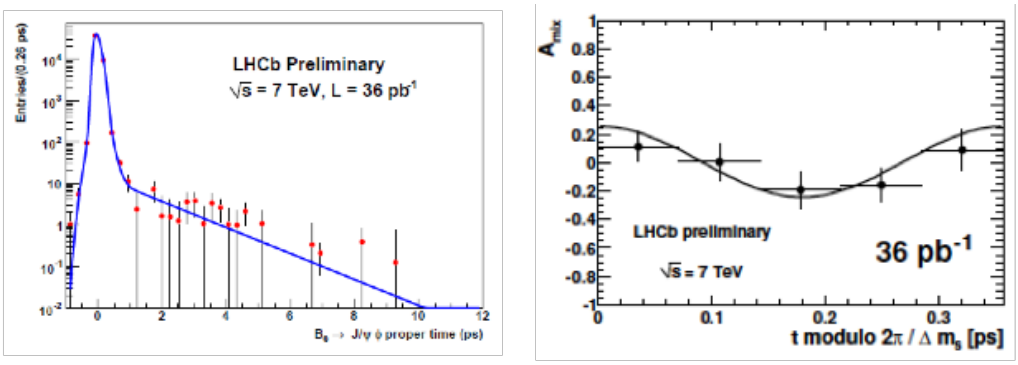

Figure 8: The left hand histogram shows the LHCb proper time distribution for the $B_s \to J/\psi\phi$ decay. The right hand histogram shows the mixing asymmetry for B_s signal candidates as a function of proper time modulo $\frac{2\pi}{\Delta m_s}$, as measured by LHCb.

2. Production of heavy flavours

Charm and bottom quarks are produced in copious amounts at hadron colliders, in particular at the LHC, which is the world′s most intense source of charm and beauty hadrons. The measurement of beauty and charm production cross setions at $\sqrt{s}$=7 TeV in the LHC detectors acceptance is of direct importance in ascertaining the sensitivities for the fundamental parameters of heavy flavour physics programme. Furthermore, knowledge of the double-differential cross sections as a function of P_T and pseudo rapidity η has its own interest in order to test theoretical models. The LHCb acceptance in the (η, P_t) plane nicely complements that of ATLAS and CMS, which cover a central region of $|\eta| < 2.5$ and rely on high P_t lepton triggers.

The b production cross section has been measured by various methods [11, 12, 13, 14] such as using samples tagged by a displaced J/ψ vertex (ATLAS, CMS, LHCb), semileptonic B decays to final states containing muons (CMS), reconstructed D meson and muon (LHCb) and fully reconstructed $J/\psi X$ final states (CMS). All measurements are compatible and reasonably well described by theoretical models. CMS recently reported the first measurement of $B\bar{B}$ angular correlations [12]. Substantial enhancement of the cross section at small opening angles has been observed as shown in Figure 9 (left).

Knowledge of the fractions of the different B species produced in pp collisions at the LHC is required for various heavy flavour physics analyses. One important example is the determination of the $BR(B_s \to \mu\mu)$, which is very sensitive to NP, where knowledge of the relative proportions of B_s and B^+ mesons is required to normalise the B_s results to the well known branching ratio $B^+ \to J/\psi K^+$. LHCb has measured the fraction of B_s produced as compared to B_d to be $f_s/f_d = 0.253 \pm 0.017^{stat} \pm 0.017^{syst} \pm 0.020^{theor}$ using hadronic and semileptonic B decays [13]. The LHCb measurement agrees well with the values determined earlier at LEP and at the Tevatron. LHCb also reported signals indicating significant B_c production [15] which looks promising for future B_c studies.

The open charm production cross sections for D^*, D, D_s mesons at the LHC have been measured by ALICE [1], ATLAS [16] and LHCb [17]. LHCb also reported the first evidence for a D^0 production asymmetry. The charm cross-section has been found to be a factor ~ 20 higher than the beauty cross section. In general data agree with theoretical predictions within large theoretical uncertainties, as shown in Figure 9 (right) for the D^+ production cross section measured by ATLAS.

The total accuracy of the current heavy flavour production measurements is dominated by the systematic error on the luminosity measurement and the track reconstruction efficiency. Thanks to the recent progress in the luminosity estimate at the LHC (currently the luminosity is known to $\sim 3.5\%$ accuracy) and a better understanding of the tracking algorithms one would expect a substantial improvement of the experimental accuracy with the analysis of larger data samples available now. This will provide an important testing ground for QCD calculation of both the absolute value and shape of the differential cross-section.

The mechanism of direct onia production in hadron collisions, including a feed-down from the decay of heavier prompt $c\bar{c}$ states, is still not well understood. Extensive studies of $J/\psi, \Upsilon$ and other quarkonia states have started by all LHC experiments in pp and heavy ion collisions. Measurements from different experiments [18, 19, 20, 21] agree well and cover the whole range

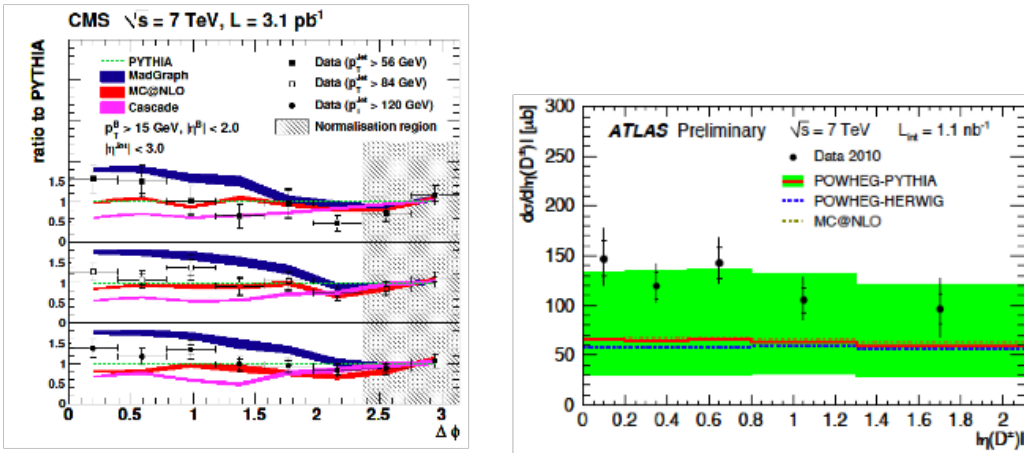

Figure 9: The left hand histogram shows the CMS measurement of the $B\bar{B}$ cross section relative to the PYTHIA prediction as function of the azimuthal angle between two B hadrons. The right hand histogram shows the ATLAS measurement of the D^+ cross section as function of the D^+ pseudo rapidity.

of rapidity as shown in Figure 10 (left). Already now, assuming a certain quarkonia polarisation, experimental data are more precise than theoretical predictions. Polarisation measurements, expected soon, will provide another powerful discriminant between models. LHCb also presented the first observation of double J/ψ production [18] at the LHC. Figure 10 (right) shows the measured cross-section as function of the invariant mass of the $J/\psi - J/\psi$ system. Larger samples are needed to make a useful comparison with theoretical predictions [22].

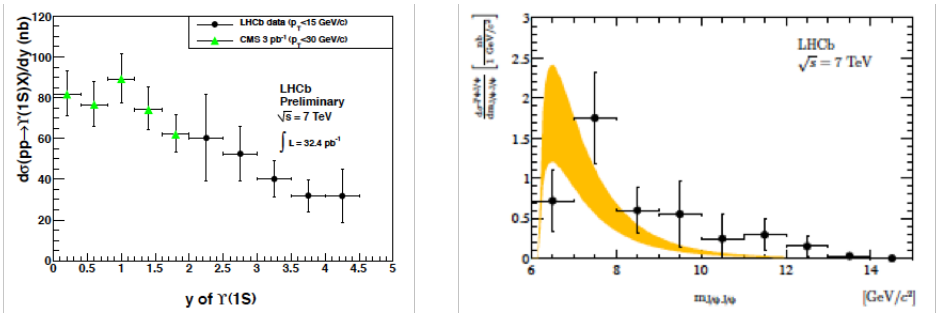

Figure 10: The left hand histogram shows the differential cross section as function of rapidity integrated over P_t, as measured by CMS and LHCb. The right hand histogram shows the differential cross section for J/ψ pairs as function of the invariant mass of the $J/\psi J/\psi$ system as measured by LHCb. The shaded area corresponds to the prediction by the model described in [22].

3. Current sensitivity to NP effects and prospects for the next few years

3.1 Measurements sensitive to NP phases

New phases in box diagrams

The most promising way to search for new phases introduced by NP to box diagrams is in the precision measurement of the B_s mixing phase ϕ_s. Within the SM this CP violating phase is

predicted very accurately and expected to be very small: $\phi_s^{SM} = -2\beta_s$. Indirect determination gives $2\beta_s = (0.0363 \pm 0.0017)$ rad [23]. Until now measurements reported by CDF and D0 [24] have had low sensitivity to this observable mainly because of the lack of statistics. LHCb has presented new constraints on ϕ_s from a tagged time-dependent angular analysis of $B_s \to J/\psi\phi$ decays using 37 pb^{-1} of integrated luminosity [6]. This LHCb measurement is less precise than the Tevatron ones because of the very low amount of integrated luminosity delivered in 2010. There are clear prospects to reach a sensitivity of ~ 0.1 rad with the 1 fb^{-1} of integrated luminosity expected by the end of 2011. The sensitivity can be further improved through inclusion of CP-eigenstate modes such as $B_s \to J/\psi f_0(980)$.

Alternatively NP contributions to box diagrams can be searched for by making a consistency test of the main Unitarity Triangle (UT). This test, well advanced by the BaBar and BELLE experiments, requires the measurement of all UT elements meaning that the exercise is more involved and less straightforward to interpret. Currently the precision of the UT elements is limited for two non-trivial sides, on account of the uncertainties of the lattice QCD inputs, and by experimental errors for the three angles.

Thanks to the B factories the angle β has been measured to a precision better than $\sim 1^\circ$, $\beta = (21.4 \pm 0.8)^\circ$ [25]. This average includes the recent world $'$ s most precise BELLE measurement, $\sin 2\beta = 0.668 \pm 0.023 \pm 0.013$, in B decays to the $J/\psi K_S^0, J/\psi K_L^0$, $\psi(2S)K_S^0$ and $\chi_{c1}K_S^0$ final states. The corresponding decay time asymmetries are shown in Figure 11. The BELLE measurement is based on the analysis of the whole available data sample of $770\times10^6 B\bar{B}$ pairs with improved track finding algorithm.

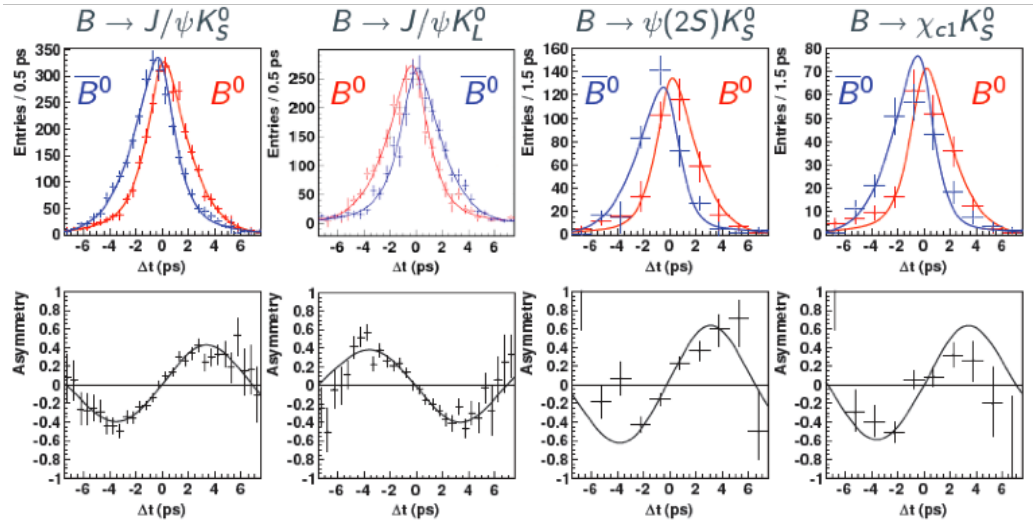

Figure 11: The plot shows decay time asymmetries for $B_d(\bar{B}_d)$ decays to the $J/\psi K_S$, $J/\psi K_L$, $\psi(2S)K_S$ and $\chi_{c1}K_S$ final states, as measured by BELLE.

The accuracy of the other two angles, α and γ, is currently rather modest, in particular for γ, where the limited statistics leads to a $\sim 20^\circ$ uncertainty [26].

Two of the five UT elements, the side opposite to the angle β and the angle γ can be extracted from the measurement of reactions explicitly described by tree diagrams, which are insensitive to NP. In contrast, the other two elements, the angle β and the side opposite to the angle γ, can

potentially receive virtual contributions from NP to box diagrams. Currently there are discrepancies observed in some measurements of UT elements at the level of a few sigma [26]. Improving the precision is important to clarify if these tensions are genuine indications of NP.

Due to the specific shape of the UT, with the angle α being close to 90°, possible contributions from NP are mainly constrained by the comparison of the angles with the opposite sides, namely β with the side proportional to $\frac{|V_{ub}|}{|V_{cb}|}$, or γ with the side proportional to $\frac{|V_{td}|}{|V_{ts}|}$. As of today both tests suffer from rather limited accuracy.

For the first pair of elements, the determination of the side is limited by $\sim 10\%$ accuracy of the $|V_{ub}|$ extraction methods [27] while for the second pair the statistical error of the angle γ measurement is by far the limiting factor. Indeed, the CKMFitter prediction extracted from direct measurements, $\gamma = (71^{+21}_{-25})^\circ$ [26], is significantly less accurate than the value arising from the global SM constraint: $\gamma = (67.9^{+4.3}_{-3.8})^\circ$ [23]. This SM constraint is mainly based on the measurement of the processes mediated by box diagrams, such as the angle β, which gives the phase of the B_d oscillation, and the side opposite to the angle γ, which is proportional to the ratio of the B_d to B_s oscillation frequencies.

Two main strategies of the angle γ measurement involve the time-independent CPV analysis of $B^+ \to D^0 K^+$ and $B^0 \to D^0 K^{*0}$ decays and the time-dependent CPV measurement of $B_s \to D_s K^+$ decays. The current status of γ measurements using the former strategy at B-factories and CDF has been summarised in [25, 28]. The accuracy of all the measurements is statistically dominated reaching for the most sensitive GGSZ method a statistical precision of $\sim 15^\circ$.

The time-dependent CPV analysis of $B_s \to D_s K^+$ decays is only applicable for experiments at hadron colliders, in particular at LHCb, which has excellent prospects to improve the precision of the time-independent measurements as well. LHCb observes clean signals in a variety of $B \to DX$ final states [29] shown in Figure 12, with yields a factor of 25 to 40 higher than corresponding yields in CDF normalised to 1 fb^{-1}, depending on the B decay channel. The combined LHCb sensitivity of the γ measurement in the 2011-2012 LHC physics run is estimated to be $\sim 5^\circ$.

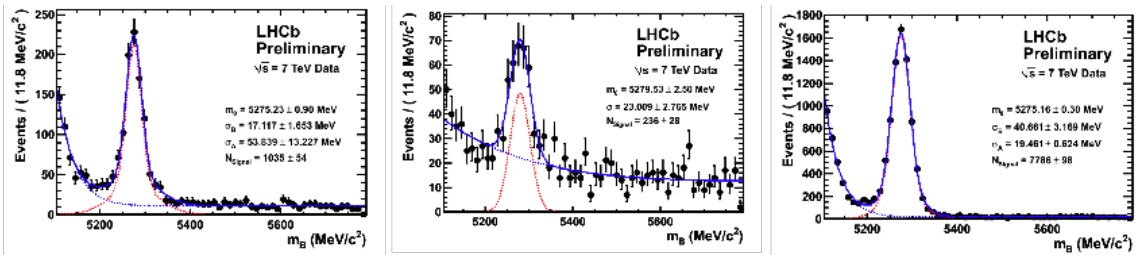

Figure 12: The plot shows the LHCb invariant mass spectra for $B^+ \to D^0(K^+K^-)\pi^+$, $B^+ \to D^0(\pi^+\pi^-)\pi^+$ and $B^+ \to D^0(\pi^+K^-)\pi^+$, as measured by LHCb.

New phases in penguin diagrams

Testing for the presence of NP phases in penguin diagrams with comparable precision to box diagrams is more challenging. The most theoretically clean measurement requires a CPV time-dependent analysis of gluonic penguins e.g. $B_s \to \phi\phi$ where the SM predicts an extremely small value of the CPV phase $\phi_s^{\phi\phi}$ [30]. Alternatively, a significant departure of $\sin 2\beta^{\phi K_s}$ measured in

$B \to \phi K_s$ decays from the already accurate value of $\sin 2\beta^{J/\psi K_s}$ would be a clear signal of a non-zero NP phase as well. Both measurements require very large data samples and most probably will have to wait for the LHCb upgrade and Super-B factories start-up.

CDF has attempted to search for the presence of NP in its sample of reconstructed $B_s \to \phi\phi$ decays (shown in Figure 13) using true CPV observables. These are experimentally accessible through the asymmetry of the functions of helicity amplitudes proportional to the interference between CP-odd and CP-even amplitudes [31]: $\mathscr{A}_v$ for transverse-longitudinal mixture and $\mathscr{A}_u$ for the transverse-transverse term. Both signal asymmetries are found to be compatible with zero within rather large uncertainties dominated by statistical errors, although the agreement for $\mathscr{A}_v$ shows a tension that approaches 2σ : $\mathscr{A}_u = (-0.7 \pm 6.4^{stat.} \pm 1.8^{syst.})\%$ and $\mathscr{A}_v = (-12.0 \pm 6.4^{stat.} \pm 1.6^{syst.})\%$ [32]. The method established by CDF needs neither tagging nor time-dependent analysis and offers an attractive opportunity to search for NP contribution to the penguin diagram with a much reduced data sample compared to that required for a time-dependent analysis.

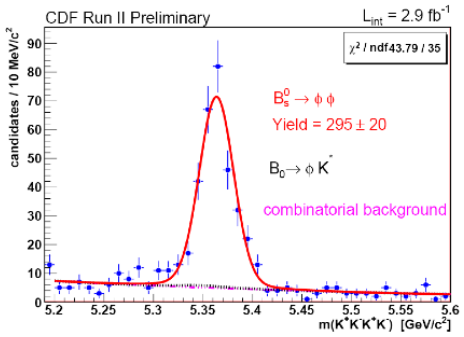

Figure 13: The plot shows the invariant mass of the $\phi\phi$ final state in the B_s region, as measured by CDF.

A contribution of NP to the penguin diagrams can also be probed through the combined measurement of time-dependent CP asymmetries in $B_d \to \pi^+\pi^-$ and $B_s \to K^+K^-$ decays [33]. This measurement is sensitive to the UT angle γ under the assumption of invariance of the strong interaction dynamics under the exchange of $d \leftrightarrow s$ quarks (so called U-spin symmetry) in two decay modes. A significant deviation from the value of γ determined in the tree mediated topologies would signal the presence of a NP phase in penguin loops. LHCb observes clean $B_d \to \pi^+\pi^-$ and $B_s \to K^+K^-$ signals as shown in Figure 6 with yields a factor of $\sim$7 exceeding those reported by CDF per 1 fb^{-1} and very little cross-feed background from other two-body B decays on account of the hadron identification provided by the RICH system.

As a first step towards time-dependent CPV studies in the charmless two-body decays, LHCb has looked for direct CPV in flavour specific final states using 37 pb^{-1} of data accumulated in 2010. Direct A_{CP} asymmetries have been extensively studied by the B factories and Tevatron. While CPV is well established in $B^0 \to K^+\pi^-$ decays, $< A_{CP} >= -0.098^{+0.012}_{-0.011}$, the corresponding measurement in $B_s \to \pi^+K^-$ by CDF, based on 1 fb^{-1} is less accurate, $A_{CP}(B_s \to \pi^+K^-) = 0.39 \pm 0.15 \pm 0.08$. LHCb has reported preliminary measurements for both asymmetries [9], as illustrated in Figure 14, $A_{CP}(B_d \to K^+\pi^-) = -0.074 \pm 0.033 \pm 0.008$ and $A_{CP}(B_s \to \pi^+K^-) = 0.15 \pm 0.19 \pm 0.02$. LHCb has also demonstrated excellent prospects for the direct CPV observation in Λ_b baryons [9].

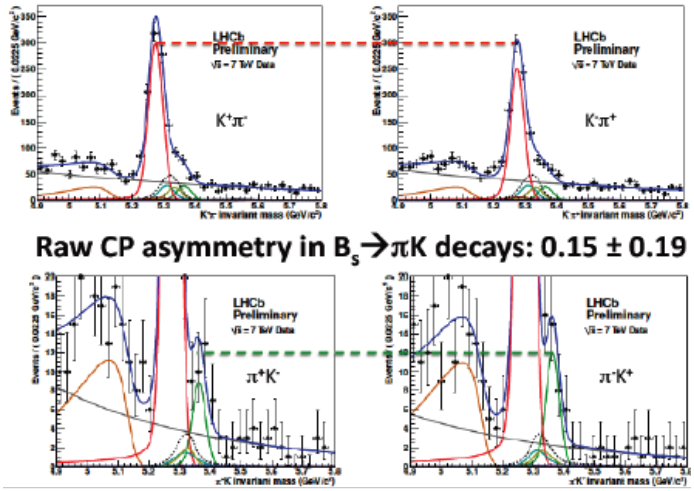

Figure 14: Top plots show the $K^+\pi^-$ (left) and $K^-\pi^+$ (right) invariant mass spectra in the $B_{d,s}$ region, as measured by LHCb. Bottom plots show the π^+K^- (left) and π^-K^+ (right) invariant mass spectra, magnified in order to focus on the two B_s signal peaks.

3.2 CPV measurements in the charm sector

Thanks to the experimental evidence for non-zero $D^0\bar{D}^0$ mixing [34], charm physics has received new attention as a powerful tool in searches for NP, in particular using CPV measurements in D mixing. This necessitates a determination of the mixing parameters x and y with improved precision since all CPV effects in mixing are governed by these parameters. Moreover, so far no single measurement has established mixing at the 5σ significance level. Mixing induced CPV asymmetries are negligible in the SM but can be enhanced in many NP models. A search for direct CPV in singly Cabibbo suppressed decays with significant contribution from gluonic penguin diagrams is another intriguing possibility to identify NP effects [35]. However a contribution from the SM accessible to experiments can not be totally excluded in this case.

CDF presented the world's most precise measurement of the time-integrated CPV asymmetry in the $D^0 \to \pi^+\pi^-$ and $D^0 \to K^+K^-$ decays based on 6 fb^{-1} of data [36]:

$$A_{CP} = \frac{\Gamma(D^0 \to h^+h^-) - \Gamma(\bar{D}^0 \to h^+h^-)}{\Gamma(D^0 \to h^+h^-) + \Gamma(\bar{D}^0 \to h^+h^-)},$$

where h stands for both π and K. The measured asymmetries, $A_{CP}(D^0 \to \pi^+\pi^-) = (+0.22 \pm 0.24 \pm 0.11)\%$ and $A_{CP}(D^0 \to K^+K^-) = (-0.24 \pm 0.22 \pm 0.10)\%$ show no evidence for CPV, which is consistent with the SM at this level of experimental sensitivity.

LHCb has demonstrated its potential for the time-dependent measurement of $y_{CP} = \frac{\tau(D^0 \to K^-\pi^+)}{\tau(D^0 \to K^+K^-)} - 1$ and $A_\Gamma = \frac{\tau(\bar{D}^0 \to K^+K^-) - \tau(D^0 \to K^+K^-)}{\tau(\bar{D}^0 \to K^+K^-) + \tau(D^0 \to K^+K^-)}$, which is the most sensitive way to search for CPV in charm mixing [37]. Using as a control channel the sample of Cabibbo favoured $D^0 \to K^-\pi^+$ decays the lifetimes of $D^0 \to K^-\pi^+$ and $\bar{D}^0 \to K^+\pi^-$ were combined in the observable

$$A_\Gamma^{K\pi} = \frac{\tau(\bar{D}^0 \to K^+\pi^-) - \tau(D^0 \to K^-\pi^+)}{\tau(\bar{D}^0 \to K^+\pi^-) + \tau(D^0 \to K^-\pi^-)},$$

which is expected to be zero. The sensitivity obtained in this control measurement, and consistency of the result with zero, provides confidence that the accuracy in y_{CP} and particularly in A_Γ will be significantly improved with 1 fb^{-1} of data collected in 2011.

LHCb also has performed a search for direct CPV through the measurement of $\Delta A_{CP} = A_{CP}(K^+K^-) - A_{CP}(\pi^+\pi^-)$ [37] using for flavour tagging the D^0 mesons produced in $D^{*+} \to D^0\pi^+$ decays. Mixing-induced CPV asymmetries, as well as production and tracking asymmetries, are expected to cancel out in ΔA_{CP} enabling a very clean measurement of direct CPV. Using 37 pb^{-1} of data LHCb has measured ΔA_{CP} to be $(-0.28 \pm 0.70^{stat} \pm 0.25^{syst})\%$. Again, a significant improvement in sensitivity is expected in 2011.

3.3 Search for NP in rare decays

Rare loop-induced B decays offer a set of experimental observables sensitive to the masses and couplings of NP. The strongest constraints on supersymmetric Higgs bosons come not from direct searches, but from limits on, and measurements of, the rates of suppressed heavy flavour decays, such as $B_s \to \mu^+\mu^-$, $b \to s\gamma$ and $B^- \to \tau^-\nu$. These observables will continue to have great importance in the era of the LHC. The current experimental sensitivity is limited by the statistics of the available data sample leaving enough room for sizable effects caused by NP contribution.

Assuming a generic coupling the inclusive measurement of $BR(b \to s\gamma)$ indirectly constraints the scale of NP masses to $\Lambda > 10^3$ TeV [38]. NP models with specific couplings can be effectively tested using exclusive rare B decays. One of the most sensitive examples is given by the super-rare $B_s \to \mu^+\mu^-$ decay. In the SM this helicity suppressed decay has a branching ratio of $BR(B_s \to \mu^+\mu^-) = (3.2 \pm 0.2) \times 10^{-9}$ [39]. In the MSSM with an extended Higgs sector $BR(B_s \to \mu^+\mu^-)$ is proportional to $\frac{\tan\beta^6}{M_A^4}$ and may significantly exceed the SM prediction for large values of the $\tan\beta$ parameter.

The best current limit from CDF, $BR(B_s \to \mu^+\mu^-) < 4.3 \times 10^{-8}$ at 95% *CL* [40], is based on the analysis of 3.7 fb^{-1} of data and still is an order of magnitude higher than the SM prediction. CDF estimated the sensitivity expected with the new improved analysis of the twice larger data sample of 7 fb^{-1}. Increased acceptance of the muon reconstruction along with better signal efficiency and background prediction should allow to reach an upper limit of 2×10^{-8} at 95% *CL*.

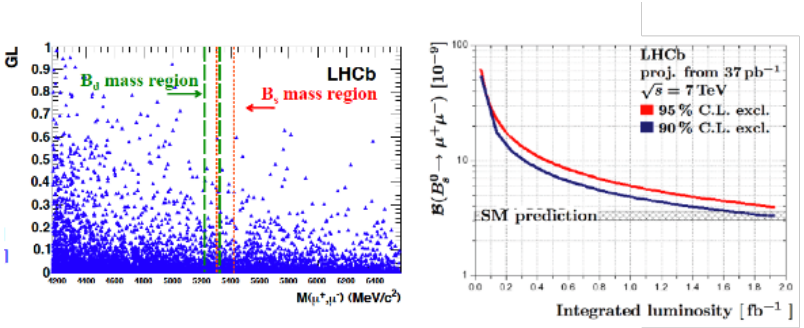

Figure 15: The left hand plot shows the two dimensional distribution of the Geometrical Likelihood versus the $\mu^+\mu^-$ invariant mass, as measured by LHCb. The right hand plot shows the LHCb exclusion limit for $BR(B_s \to \mu^+\mu^-)$ as a function of the integrated luminosity.

LHCb reported a search for $B_s \to \mu^+\mu^-$ decays with a data sample of 37 pb^{-1} [10]. The analysis has been performed in bins of the $\mu^+\mu^-$ invariant mass and a Geometrical Likelihood GL, which combines information related to event topology and kinematics. The GL distribution is flat for signal events and falls exponentially for background events. As seen in Figure 15 (left) LHCb observes no events in the signal region for the most sensitive GL bins leading to an upper limit $BR(B_s \to \mu^+\mu^-) < 5.6 \times 10^{-8}$ at 95% *CL*. The LHCb prospects to exclude a $B_s \to \mu^+\mu^-$ signal down to a certain branching ratio are shown in Figure 15 (right) as a function of accumulated integrated luminosity.

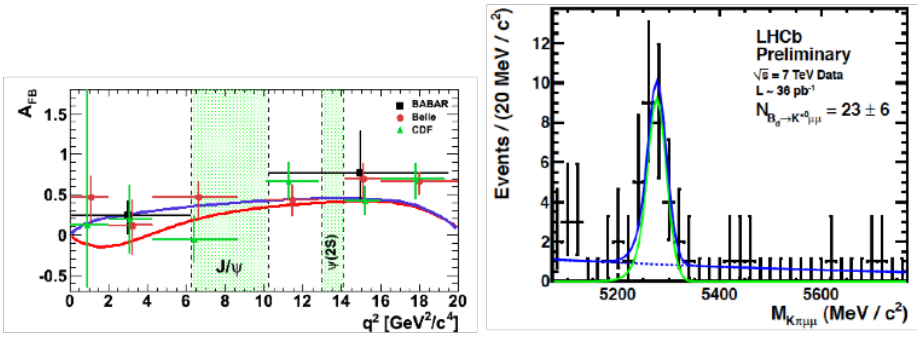

Figure 16: The left hand plot summarises the measurements of the forward-backward asymmetry in $B_d \to K^*\mu^+\mu^-$ decays by BABAR, BELLE and CDF. The right hand histogram shows the signal for $B_d \to K^*\mu^+\mu^-$ decays, as measured by LHCb.

Several strategies have been proposed to search for NP effects in the processes mediated by radiative and electroweak penguin diagrams through the measurement of the helicity structure of the inherent amplitudes [42]. Owing to the $V-A$ structure of the W-boson coupling, the photon produced in $b \to s\gamma$ transitions is predominantly left-handed up to corrections of order $\frac{m_s}{m_b}$, which arise from a chirality flip. The decay $B_d \to K^{*0}\mu^+\mu^-$ proceeds via a combination of the electroweak penguin and box diagrams. The FCNC describing this $b \to s$ transition contains a right-handed component that is well calculable in the SM but can be affected by NP contributions resulting in modified angular distributions. As an example, the forward-backward asymmetry, $A^{FB}(q^2 = m^2_{\mu\mu})$, is particularly sensitive to NP contributions at its zero-point, s_0, since the dominant theoretical uncertainty from hadronic form-factors cancels out at leading order.

First measurements of the forward-backward asymmetry, shown in Figure 16 (left), have been made by the B-factories and CDF [41], with results providing an intriguing hint of a deviation from the SM prediction. A clean signal for $B_d \to K^*\mu^+\mu^-$ decay reconstructed at LHCb [10] with a data sample of 36 pb^{-1} is shown in Figure 16 (right). LHCb should be able to clarify the existing situation and provide an accurate measurement of A^{FB} zero crossing point with the $\sim$1 fb^{-1} data sample expected in 2011.

4. Conclusion

The impressive start-up of the LHC experiments certainly allows flavour physics to access a new level of quality. The data sample of $\sim$40 pb^{-1} accumulated in 2010 by the LHC detectors was sufficient to measure *c*-, *b*- and *onia* production cross sections and observe significant signal peaks

in a large fraction of the key decay modes of the flavour physics programme. The event yields and detector resolutions are similar to those expected from simulation, showing that the trigger and tracking are performing as expected. The background level is satisfactory in all cases. CDF and D0 nonetheless remain at the forefront of flavour physics by taking advantage of their fully understood detectors and analysis techniques. The update of many Tevatron analyses with the full available data sample is expected in the near future. New exciting results have been reported by the B-factories in the sector of heavy flavour spectroscopy.

The current LHC plan foresees a two-year physics run at the centre-of-mass energy of $\sim$7 TeV in order to collect a data sample of $\sim$5 fb^{-1} data for ATLAS and CMS, and $\sim$2 fb^{-1} data for LHCb. LHCb will certainly reach a new level of sensitivity in the flavour physics "golden" measurements of the B_s mixing phase and $BR(B_s \to \mu^+\mu^-)$, as well as the angular analysis of the $B_d \to K^*\mu^+\mu^-$ decays, opening exciting prospects for discoveries. ATLAS and CMS will provide competitive results for $BR(B_s \to \mu^+\mu^-)$ taking advantage of their larger data samples. High class measurements for the study of *CP* violation in the charm sector give another promising possibility to discover NP effects.

In summary, high precision tests of the SM are guaranteed already in 2011-2012. This may lead to either a discovery of NP effects or will put strong constraints on the NP models. Further exploration of flavour physics in the more distant future requires the upgrade of the LHCb experiment [43] at CERN and construction of the SuperKEKB [44] in Japan, and SuperB [45] in Italy.

References

[1] B. Giuseppe, *Open heavy flavour measurements with the ALICE experiment at the LHC*, Proceedings of this conference.

[2] R. Nikolaidou, *ATLAS detector performance*, Proceedings of this conference.

[3] H. Snoek, *CMS detector performance*, Proceedings of this conference.

[4] N. Harnew, *LHCb detector performance*, Proceedings of this conference.

[5] S. Vecchi, *Flavour tagging and mixing at LHCb*, Proceedings of this conference.

[6] U. Uwer, $B_s \to J/\psi\phi$ *at LHCb*, Proceedings of this conference.

[7] A. Dewhurst, $B_s \to J/\psi\phi$ *at ATLAS*, Proceedings of this conference.

[8] V. Azzolini, *Studies of the* B_s *in* $J/\psi\phi$ *decay with CMS*, Proceedings of this conference.

[9] V. Vagnoni, $B \to hh$ *(hadronic final states - LHCb*, Proceedings of this conference.

[10] M. Palutan, *Rare decay results and prospects with LHCb*, Proceedings of this conference.

[11] I. Christidi, *Open b and* $b\bar{b}$ *cross section using inclusive and exclusive channels at ATLAS*, Proceedings of this conference.

[12] C. Grab, *Beauty production results from CMS*, Proceedings of this conference.

[13] N. Tuning, *b production cross section and fragmentation fractions at LHCb*, Proceedings of this conference.

[14] E. Aguilo, *Measurement of exclusive B-hadron production at 7 TeV with the CMS experiment*, Proceedings of this conference.

[15] J. He, *J/ψ and B_c production at LHCb*, Proceedings of this conference.

[16] S. Head, *D meson production cross section - ATLAS*, Proceedings of this conference.

[17] A. Kozlinsky, *Charm production at LHCb*, Proceedings of this conference.

[18] J. Cogan, *Quarkonia studies in LHCb: $\Upsilon(1S)$, Double J/ψ, $\psi(2S)$, χ_c*, Proceedings of this conference.

[19] M. Corradi, *Dimuon reconstruction for B-physics in ATLAS*, Proceedings of this conference.

[20] S.-C. Hsu, *J/ψ production in pp and in heavy-ions collisions in ATLAS*, Proceedings of this conference.

[21] N. Leonardo, *Measurement of $\Upsilon(nS)$ and J/ψ production at 7 TeV - CMS*, Proceedings of this conference.

[22] A.V. Berezhnoy, A.K. Likhoded, A.V. Luchinsky and A.A. Novoselov, *Double J/ψ meson production at LHC and 4c - tetraquark state*, arXiv: 1101.5881 [hep-ph].

[23] J. Charles *et al.* (CKMfitter group), Eup. Phys. J. C41, 1-131 (2005), hep-ph/0406184, updated results and plots available at http://ckmfitter.in2p3.fr.

[24] I. Ripp-Baudot, *CP violation measurements with $B_s \to J/\psi\phi$ decays at the Tevatron*, Proceedings of this conference.

[25] M. Rohrken, *Unitarity Triangle measurements - BaBar/BELLE*, Proceedings of this conference.

[26] H. Lacker, *Status of the Unitarity Triangle*, Proceedings of this conference.

[27] B. Kowalewski, *$|V_{ub}$ and $|V_{cb}|$ from semileptonic B decays and $B \to \tau\nu$*, Proceedings of this conference.

[28] P. Garosi, *First ADS analysis of $B^+ \to D^0K$ decays in hadronic collisions at CDF*, Proceedings of this conference.

[29] S. Blusk, *$B_s \to D_sh$ and $B \to Dh$ decays in LHCb*, Proceedings of this conference.

[30] M. Raidal, Phys. Rev. Lett. 89 (2002) 231803.

[31] J. Rosner, *B_s decays and mixing*, Proceedings of this conference.

[32] M. Dorigo, *Suppressed B_s decays - Tevatron*, Proceedings of this conference.

[33] R. Fleisher, Phys. Lett. B 459 (1999) 306, R. Fleisher, Eur. Phys. J. C 52 (2007) 267.

[34] Heavy Flavour Averaging Group, arXiv: 1101.1589 [hep-ex].

[35] Y. Grossman, A.L. Kagan and Y. Nir, Phys. Rev. D 75.

[36] A. Di Canto, *Searching for New Physics through charm at CDF*, Proceedings of this conference.

[37] M. Gersabeck, *Charm mixing and CP violation at LHCb*, Proceedings of this conference.

[38] Y. Nir, Nucl. Phys. Proc. Suppl. 117 (2003) 111.

[39] A.J. Buras, arXiv:1012.1447, E. Gamiz *et al.*, Phys. Rev. D 80 (2009), A.J. Byras, Phys. Lett. B256 (2003) 115.

[40] D. Kong, *Rare decays at the Tevatron*, Proceedings of this conference.

[41] B. Aubert *et al.* (BABAR Collaboration), Phys. Rev. D 79 (2009) 031102, J.T. Wei *et al.* (BELLE Collaboration), Phys. Rev. Lett. 103 (2009) 171801, T. Altonen *et al.* (CDF Collaboration), arXiv:1101.1028 [hep-ex].

[42] See for a review T. Hurth and M. Nakao, Ann. Rev. Nucl. Part. Sci. 60 (2010) 645.

[43] M. Merk, *LHCb Upgrade*, Proceedings of this conference.

[44] J. Brodzicka, *SuperKEKB*, Proceedings of this conference.

[45] F. Wilson, *SuperB*, Proceedings of this conference.